Eigenstructure Analysis from Symmetrical Graph Motives with Application to Aggregated Controller Design

Takayuki Ishizaki[1], Risong Ku[1], and Jun-ichi Imura[1]

Abstract— **In this paper, we analyze the eigenstructure of network systems having symmetrical graph motives and apply it to reduced order controller design based on their aggregated models. In the eigenstructure analysis, formulating the symmetry of graph motives as the graph automorphism, we show that particular eigenspace decomposition of network systems can be found by analyzing the common eigenspaces of all possible permutation matrices, with regard to the graph automorphism. This eigenspace decomposition explains the appearance of uncontrollable and unobservable subspaces that can be removed by aggregating, i.e., averaging, symmetrical graph motives. Furthermore, it turns out that the resultant aggregated model, whose state behavior tracks a kind of centroids of that of the original network system, has good compatibility with observer-based state feedback controller design. The efficiency of the aggregated controller design method is numerically demonstrated by output regulation of second-order oscillator networks.**

I. Introduction

Many of network systems found in the real world have been shown to share several common characteristics, e.g., the small-world property, the scale-free property, high cluster coefficients, and so forth [1], [2]. Besides them, some particular patterns of interconnections, called network motives or graph motives, can often be found [3], [4]. Graph motives correspond to recurring subnetworks, which can naturally appear as network growth with duplication [5]. This kind of duplication endows resultant networks with geometrical symmetry in the sense that the permutation of graph motives leave the entire network invariant.

In this paper, formulating the symmetry of graph motives as the graph automorphism [6], we first analyze the eigenstructure of network systems having symmetrical graph motives. On the basis of the fact that the simultaneous diagonalizability of square matrices is equivalent to the commutativity of multiplication [7], we show that particular eigenspace decomposition of network systems can be found by analyzing the common eigenspaces of all possible permutation matrices that leave networks invariant. Our result is deduced purely from the symmetry of graph motives; The analysis based on the simultaneous diagonalizability makes no distinction among directed and undirected graphs, adjacency and graph Laplacian matrices, and others [8]. From this viewpoint, our analysis can be seen to be more universal than those in [9], [10], each of which focuses on adjacency and graph Laplacian matrices.

[1]Department of Mechanical and Environmental Informatics, Graduate School of Information Science and Engineering, Tokyo Institute of Technology; 2-12-1, Meguro, Tokyo, Japan.
`{ishizaki,ku,imura}@cyb.mei.titech.ac.jp`

Furthermore, as an application of the eigenstructure analysis, we develop a reduced order controller design method that makes use of a reduced order model obtained by aggregating symmetrical graph motives. This method is based on the fact that the existence of symmetrical graph motives makes a local state space associated with the motives both uncontrollable and unobservable, when the input and output ports are assigned to nodes other than the motives. It will turn out that an aggregated model given by removing the redundant state spaces has good compatibility with state feedback controller design based on average state observation, which tracks a kind of centroids of the system states. The efficiency of this aggregated controller design method is numerically demonstrated by output regulation of second-order oscillator networks, which are often used as a primary model of rotary appliances in power systems control [11].

To clarify our contribution, we provide some references on the controllability analyses of network systems. In the line of works [12], [13], a controllability analysis based on the equitable partition is performed for single-leader leader-follower networks with a consensus protocol. In particular, a condition to make network systems *completely controllable* is derived in view of graph symmetry from the equitable partition. Most of network controllability analyses, e.g., [14], focus on the discussion of complete controllability, i.e., the ability to steer the states to an *arbitrary* place. It should be noted that this complete controllability is not necessarily realistic for the control of large-scale network systems. For example, in power systems control, it is not necessarily reasonable to individually handle a large number of generators from the viewpoint of operation and implementation costs. In this sense, the complete controllability is generally strict and excessive for the control of large-scale network systems.

On the other hand, for large-scale network systems, we are not always interested in the exact steering of individual state variables towards individual target values, but we are only interested in the control of a kind of macroscopic behavior, e.g., the centroids (averages) of node groups classified with respect to synchronism among nodes [15]–[17]. As being compatible with this viewpoint, our aggregated controller design is performed on the premise that the network systems of interest involve a number of symmetrical graph motives whose states are to be synchronized with each other. This can be viewed as the case where they involve a number of stable uncontrollable and unobservable modes corresponding to the disagreement with the average of the state space associated with the motives. As long as the input and output ports are assigned to make their aggregated model controllable and observable, we can design the aforementioned aggregated controller in a systematic manner. Through the arguments in this paper, we aim at showing that making explicit use of the redundancy from graph symmetry, i.e., the existence of particular stable modes that are both uncontrollable and unobservable, can be a key insight into performing reasonable control system design that is scalable to large-scale network systems.

The rest of this paper is organized as follows. In Section II, we first provide the system description of dynamical networks having symmetrical graph motives. In Section III, we analyze the eigenstructure of the network systems from the viewpoint of the graph automorphism and then apply the analysis to reduced order controller design based on their aggregated models. Section IV demonstrates the efficiency of our aggregated controller design method numerically. Finally, Section V provides concluding remarks of this paper.

Notation: We denote the identity matrix by I, the all-ones vector by $\boldsymbol{1}$, the image of a matrix A by $\mathrm{im}\, A$, the kernel by $\ker A$, the block diagonal matrix whose diagonal blocks are A and B by $\mathrm{diag}(A, B)$, the Kronecker product of A and B by $A \otimes B$, the set of eigenvalues of A by $\mathrm{spec}(A)$, the orthogonal complement of a subspace $\mathcal{V}$ by $\mathcal{V}^{\perp}$, the column vector stacking a set of vectors x_i by $\mathrm{col}(x_1, \ldots, x_n)$, and the subspace spanned by x_i by $\mathrm{span}\{x_1, \ldots, x_n\}$. A pair (λ, v) is said to be an eigenpair of A if $Av = \lambda v$ holds. A subspace $\mathcal{V}$ is said to be an eigenspace of A associated with an eigenvalue λ if $\mathcal{V} \subseteq \ker \lambda I - A$.

Let $\mathcal{V}_1$ and $\mathcal{V}_2$ be subspaces of a vector space. The sum of $\mathcal{V}_1$ and $\mathcal{V}_2$ is denoted by

$$\mathcal{V}_1 + \mathcal{V}_2 := \{x_1 + x_2 : x_1 \in \mathcal{V}_1,\ x_2 \in \mathcal{V}_2\},$$

which may be rewritten as $\sum_{i \in \{1,2\}} \mathcal{V}_i$. The union is denoted by

$$\mathcal{V}_1 \cup \mathcal{V}_2 := \{x : x \in \mathcal{V}_1 \text{ or } x \in \mathcal{V}_2\},$$

which may be rewritten as $\bigcup_{i \in \{1,2\}} \mathcal{V}_i$, and the intersection is denoted by

$$\mathcal{V}_1 \cap \mathcal{V}_2 := \{x : x \in \mathcal{V}_1 \text{ and } x \in \mathcal{V}_2\},$$

which may be rewritten as $\bigcap_{i \in \{1,2\}} \mathcal{V}_i$.

II. System Description

In this paper, we consider a linear network system evolving over graphs described by

$$\boldsymbol{\Sigma} : \begin{cases} \dot{\boldsymbol{x}} = \boldsymbol{A}\boldsymbol{x} + \boldsymbol{B}\boldsymbol{u}, & \boldsymbol{x}(0) = \boldsymbol{x}_0 \\ \boldsymbol{y} = \boldsymbol{C}\boldsymbol{x} \end{cases} \tag{1}$$

where the system matrices are supposed to be structured as

$$\begin{aligned} \boldsymbol{A} &= \begin{bmatrix} A_0 & H_0(\boldsymbol{1}^{\mathsf{T}} \otimes F) \\ (\boldsymbol{1} \otimes H)F_0 & I \otimes A + \mathit{\Gamma} \otimes BC \end{bmatrix}, \\ \boldsymbol{B} &= \begin{bmatrix} B_0 \\ 0 \end{bmatrix}, \quad \boldsymbol{C} = \begin{bmatrix} C_0 & 0 \end{bmatrix}. \end{aligned} \tag{2}$$

In this formulation, the second half dynamics corresponds to the network of a set of graph motives having the same dynamics, whose interconnection structure is represented by $\mathit{\Gamma}$, whereas the first half dynamics corresponds to the remaining part other than the graph motives. The details are explained through the following example.

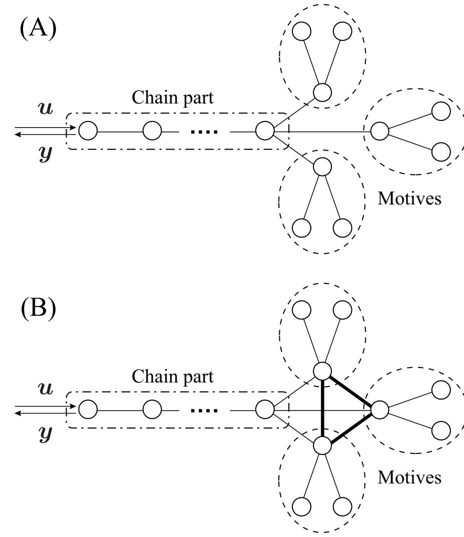

Fig. 1. Examples of chain graph with three motives.

Example: Let us consider the dynamics based on the adjacency matrices of the two graphs in Figs. 1-(A) and (B). Both are composed of a chain graph with three graph motives, depicted by the dashed-dotted line and dashed lines, respectively. The system matrices of the chain part are given as follows. The state transition matrix A_0 is the tridiagonal matrix whose superdiagonal and subdiagonal elements are all one. The input and output matrices are given as

$$B_0 = C_0^{\mathsf{T}} = \mathrm{col}(1, 0, \ldots, 0), \quad H_0 = F_0^{\mathsf{T}} = \mathrm{col}(0, \ldots, 0, 1),$$

which correspond to the input and output nodes with the external signals $\boldsymbol{u}$ and $\boldsymbol{y}$ and the interconnection with the motives, respectively. On the other hand, the dynamics of the motives is described by

$$A = \begin{bmatrix} 0 & 1 & 1 \\ 1 & 0 & 0 \\ 1 & 0 & 0 \end{bmatrix}, \quad B = H = C^{\mathsf{T}} = F^{\mathsf{T}} = \begin{bmatrix} 1 \\ 0 \\ 0 \end{bmatrix},$$

where B and C are relevant to the interconnection among motives, and H and F are relevant to the interconnection with the chain part. The difference between the graphs in Figs. 1-(A) and (B) appears in the interconnection matrices, which are given as

$$\mathit{\Gamma} = 0, \quad \mathit{\Gamma} = \begin{bmatrix} 0 & 1 & 1 \\ 1 & 0 & 1 \\ 1 & 1 & 0 \end{bmatrix}, \tag{3}$$

respectively. The cases of e.g., directed graphs, edge-weighted networks, and graph Laplacian matrices can be considered in a similar manner. $\square$

In this paper, we first analyze the eigenstructure of $\boldsymbol{A}$ in (2) deduced from the existence of symmetrical graph motives, and then apply the analysis to aggregated controller design for the network system $\boldsymbol{\Sigma}$ in (1).

III. Eigenstructure Analysis

A. Eigenstructure from Symmetrical Graph Motives

In this subsection, we investigate a general principle of the structure of eigenspaces of $\boldsymbol{A}$ in (2) that is deduced from symmetrical graph motives. This eigenstructure analysis is dependent on the symmetry of $\mathit{\Gamma}$, but not reliant on the specific choices of system matrices in (2).

An interconnection matrix $\mathit{\Gamma}$ is said to be *symmetrical* with respect to a permutation matrix $\mathit{\Pi}$ if

$$\mathit{\Pi}\mathit{\Gamma} = \mathit{\Gamma}\mathit{\Pi}. \tag{4}$$

We denote the set of all permutation matrices that satisfy (4) by $\mathbb{P}[\mathit{\Gamma}]$, in which we do not include the identity matrix without loss of generality. This is called the graph automorphism [6]. From (4), we have $\mathit{\Pi}\mathit{\Gamma}\mathit{\Pi}^{\mathsf{T}} = \mathit{\Gamma}$, implying that interchanging a set of indices, compatible with a node set having symmetry, makes no change in the matrix $\mathit{\Gamma}$. For example, both interconnection matrices $\mathit{\Gamma}$ in (3) are symmetrical with respect to any permutation matrix. Note that this definition of symmetry makes no distinction between directed and undirected graphs as well as adjacency and graph Laplacian matrices. Furthermore, $\mathit{\Pi}\mathit{\Gamma}^{\mathsf{T}} = \mathit{\Gamma}^{\mathsf{T}}\mathit{\Pi}$ is also led by (4).

From $\mathit{\Pi}\boldsymbol{1} = \boldsymbol{1}$, we can verify that

$$\boldsymbol{\Pi}\boldsymbol{A} = \boldsymbol{A}\boldsymbol{\Pi}, \quad \boldsymbol{\Pi} := \mathrm{diag}(I, \mathit{\Pi} \otimes I), \tag{5}$$

which implies that $\boldsymbol{A}$ is symmetrical with respect to the permutation matrix $\boldsymbol{\Pi}$. It is known that square matrices are simultaneously diagonalizable if and only if they commute [7]. From this fact, we see that $\mathit{\Pi}$ and $\mathit{\Gamma}$ in (4) share the same eigenvectors, as well as $\boldsymbol{\Pi}$ and $\boldsymbol{A}$ in (5) do so. Therefore, the eigenspaces of $\boldsymbol{A}$ can be deduced from the analysis of $\boldsymbol{\Pi}$. In the following, we assume that the square matrices, e.g., $\boldsymbol{A}$ and $\mathit{\Gamma}$, are all diagonalizable.

Because $\boldsymbol{\Pi}$ is unitary for any $\mathit{\Pi} \in \mathbb{P}[\mathit{\Gamma}]$, the eigenvalues of $\boldsymbol{\Pi}$ locate on the unit circle in the complex plane and their eigenvectors can form an orthogonal basis. From the block diagonal structure of $\boldsymbol{\Pi}$ in (5), we see that the eigenvector v of $\boldsymbol{\Pi}$ associated with the multiple eigenvalues of $\pi = 1$ lies in the space of

$$v \in \mathrm{im}\begin{bmatrix} I \\ 0 \end{bmatrix} + \mathrm{im}\begin{bmatrix} 0 \\ w \otimes I \end{bmatrix} \tag{6}$$

where w is an eigenvector of $\mathit{\Pi}$ associated with the multiple eigenvalues of $\pi = 1$. On the other hand, the eigenvector v of $\boldsymbol{\Pi}$ associated with $\pi \in \mathrm{spec}(\boldsymbol{\Pi}) \setminus \{1\}$ lies in the space of

$$v \in \mathrm{im}\begin{bmatrix} 0 \\ \overline{w} \otimes I \end{bmatrix} \tag{7}$$

where $\overline{w}$ is an eigenvector associated with $\pi \in \mathrm{spec}(\mathit{\Pi}) \setminus \{1\}$. Thus we see that the eigenspace analyses of $\mathit{\Pi}$ can be divided into the cases of $\pi = 1$ and $\pi \neq 1$.

First we show the following result deduced by analyzing the eigenspaces of $\mathit{\Pi} \in \mathbb{P}[\mathit{\Gamma}]$ associated with $\pi = 1$.

Theorem 1: Let $\mathit{\Gamma}$ be symmetrical. If

$$\bigcap_{\mathit{\Pi} \in \mathbb{P}[\mathit{\Gamma}]} \ker I - \mathit{\Pi} = \mathrm{span}\{\boldsymbol{1}\}, \tag{8}$$

then, for any eigenvalue of $\mathit{\Gamma}$, there exists an associated eigenvector w such that

$$w \in \mathrm{span}\{\boldsymbol{1}\} \cup \mathrm{span}\{\boldsymbol{1}\}^{\perp}. \tag{9}$$

Proof: Let q be the number of permutation matrices that belong to $\mathbb{P}[\mathit{\Gamma}]$. Denote $\mathcal{V}_i := \ker I - \mathit{\Pi}_i$ for $i = 1, \ldots, q$. Note that

$$\mathcal{V}_i^{\perp} \subseteq \mathrm{span}\{\boldsymbol{1}\}^{\perp} \tag{10}$$

because the eigenvectors associated with $\pi \in \mathrm{spec}(\mathit{\Pi}_i) \setminus \{1\}$ are orthogonal to the eigenspace $\mathrm{span}\{\boldsymbol{1}\}$ associated with $\pi = 1$, namely

$$\mathcal{V}_i^{\perp} = \textstyle\sum_{\pi \in \mathrm{spec}(\mathit{\Pi}_i) \setminus \{1\}} \ker \pi I - \mathit{\Pi}_i.$$

Furthermore, it follows that each of eigenvectors of $\mathit{\Gamma}$ lies in either $\mathcal{V}_i$ or $\mathcal{V}_i^{\perp}$, because $\mathit{\Pi}_i$ and $\mathit{\Gamma}$ are simultaneously diagonalizable. Consider an eigenvector $w \in \mathcal{V}_i$ of $\mathit{\Gamma}$. Then we see that

$$w \in (\mathcal{V}_i \cap \mathcal{V}_j) \cup \left(\mathcal{V}_i \cap \mathcal{V}_j^{\perp}\right), \quad \forall j = 1, \ldots, q.$$

If $w \in \mathcal{V}_i \cap \mathcal{V}_j^{\perp}$ for some j, then $w \in \mathrm{span}\{\boldsymbol{1}\}^{\perp}$ because of (10). On the other hand, if $w \notin \mathcal{V}_i \cap \mathcal{V}_j^{\perp}$ for all j, then

$$w \in \textstyle\bigcap_{j \in \{1,\ldots,q\}} \mathcal{V}_j = \mathrm{span}\{\boldsymbol{1}\}$$

owing to (8). This proves the claim. ■

Theorem 1 shows that the eigenspaces of an interconnection matrix $\mathit{\Gamma}$ satisfying (8) is decomposed as in (9). In the rest of this paper, an interconnection matrix $\mathit{\Gamma}$ is said to be *strictly symmetrical* if (8) holds. One may think that the eigenvectors of a graph Laplacian matrix always admit the decomposition of (9). However, note that Theorem 1 is deduced from only the symmetry in the sense of (4), whose definition makes no distinction among adjacency and graph Laplacian matrices and other details.

Example: Both interconnection matrices of $\mathit{\Gamma}$ in (3) are strictly symmetrical. This can be easily verified because they are symmetrical with respect to any permutation matrices, including the circulant permutation matrix given as

$$\mathit{\Pi} = e_1 e_2^{\mathsf{T}} + e_2 e_3^{\mathsf{T}} + \cdots + e_{\nu} e_1^{\mathsf{T}}, \tag{11}$$

where e_i denotes the ith unit vector and ν denotes the size of $\mathit{\Pi}$. Since the eigenvectors of this permutation matrix coincides with the discrete Fourier transform vectors [18], it satisfies $\ker I - \mathit{\Pi} = \mathrm{span}\{\boldsymbol{1}\}$, which is sufficient for (8). Furthermore, we see that any interconnection matrix $\mathit{\Gamma}$ being circulant, e.g., in the left of Fig. 2, is strictly symmetrical, because all circulant matrices commute.

Next let us consider an interconnection matrix of

$$\mathit{\Gamma} = \begin{bmatrix} \gamma_1 & \beta & \beta \\ \beta & \gamma_2 & 0 \\ \beta & 0 & \gamma_2 \end{bmatrix}, \tag{12}$$

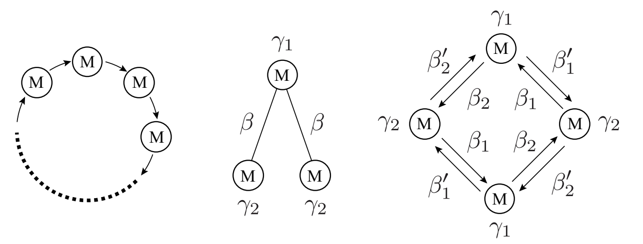

Fig. 2. Examples of symmetrical interconnection structure, where the motives are denoted by "M".

which is depicted in the center of Fig. 2. We can easily verify that this $\varGamma$ is symmetrical with respect to the single permutation matrix

$$\varPi = \mathrm{diag}(1, \overline{I}), \quad \overline{I} := \begin{bmatrix} 0 & 1 \\ 1 & 0 \end{bmatrix}. \tag{13}$$

Thus we obtain

$$\ker I - \varPi = \mathrm{span}\left\{ \mathrm{col}(1,0,0),\ \mathrm{col}(0,1,1) \right\}. \tag{14}$$

This shows that $\varGamma$ in (12) is not classified into strictly symmetrical matrices, even though a particular case, e.g., the symmetric graph Laplacian matrix given as $\gamma_1 = -2\beta$ and $\gamma_2 = -\beta$, admits the property of (9).

Finally, let us consider the case of

$$\varGamma = \left[\begin{array}{cc|cc} \gamma_1 & \beta_1 & 0 & \beta'_2 \\ \beta'_1 & \gamma_2 & \beta_2 & 0 \\ \hline 0 & \beta_2 & \gamma_1 & \beta'_1 \\ \beta'_2 & 0 & \beta_1 & \gamma_2 \end{array} \right], \tag{15}$$

which is depicted in the right of Fig. 2; a similar example can be found in [10]. If $\gamma_1 = \gamma_2$, $\beta_1 = \beta'_1$, and $\beta_2 = \beta'_2$, we have

$$\mathbb{P}[\varGamma] = \left\{ \begin{bmatrix} 0 & I \\ I & 0 \end{bmatrix}, \begin{bmatrix} \overline{I} & 0 \\ 0 & \overline{I} \end{bmatrix}, \begin{bmatrix} 0 & \overline{I} \\ \overline{I} & 0 \end{bmatrix} \right\}, \tag{16}$$

otherwise

$$\mathbb{P}[\varGamma] = \left\{ \begin{bmatrix} 0 & I \\ I & 0 \end{bmatrix} \right\}.$$

Then the term in the left-hand side of (8) is given as

$$\bigcap_{\varPi \in \mathbb{P}[\varGamma]} \ker I - \varPi = \mathrm{im} \begin{bmatrix} I \\ I \end{bmatrix} \cap \mathrm{im}\, I \otimes \begin{bmatrix} 1 \\ 1 \end{bmatrix} \cap \mathrm{im} \begin{bmatrix} I \\ \overline{I} \end{bmatrix}$$

for the former case, which is equal to $\mathrm{span}\{\boldsymbol{1}\}$, while it is given as

$$\bigcap_{\varPi \in \mathbb{P}[\varGamma]} \ker I - \varPi = \mathrm{im} \begin{bmatrix} I \\ I \end{bmatrix}$$

for the latter case. Thus $\varGamma$ in (15) is strictly symmetrical only in the former case. Note that this strict symmetry is inherent in $\varGamma$ with arbitrary choice of the parameters γ_i and β_i. $\square$

On the basis of Theorem 1, which shows the eigenspace decomposition of $\varGamma$ led by analyzing the eigenspaces of $\varPi$ associated with $\pi = 1$, we next analyze the eigenspaces of $\boldsymbol{A}$ in (2). Owing to the commutativity of (5), the decomposition of eigenspaces of $\boldsymbol{A}$ can be deduced from the strict symmetry of $\varGamma$ as follows.

Theorem 2: Consider $\boldsymbol{A}$ in (2) with $\varGamma$ being strictly symmetrical. Then, for any eigenvalue of $\boldsymbol{A}$, there exists an associated eigenvector v such that

$$v \in \left(\mathrm{im} \begin{bmatrix} I \\ 0 \end{bmatrix} + \mathrm{im} \begin{bmatrix} 0 \\ \boldsymbol{1} \otimes I \end{bmatrix} \right) \cup \mathrm{im} \begin{bmatrix} 0 \\ w \otimes I \end{bmatrix} \tag{17}$$

where w is an eigenvector of $\varGamma$ such that $w \in \mathrm{span}\{\boldsymbol{1}\}^{\perp}$.

Proof: From (5), we see that the eigenvectors of $\boldsymbol{A}$ can be classified into (6) and (7). Because $\varGamma$ is assumed to be strictly symmetrical, its eigenvector can also be classified as shown in Theorem 1. Thus w in (6) satisfies $w \in \mathrm{span}\{\boldsymbol{1}\}$ whereas $\overline{w}$ in (7) satisfies $\overline{w} \in \mathrm{span}\{\boldsymbol{1}\}^{\perp}$.

Let $(\lambda_\gamma, v_\gamma)$ be an eigenpair of $A + \gamma BC$ for $\gamma \in \mathrm{spec}(\varGamma)$ associated with an eigenvector $\overline{w} \in \mathrm{span}\{\boldsymbol{1}\}^{\perp}$. Then we have

$$\boldsymbol{A}\,\mathrm{col}(0, \overline{w} \otimes v_\gamma) = \lambda_\gamma \mathrm{col}(0, \overline{w} \otimes v_\gamma),$$

which shows that $\mathrm{col}(0, \overline{w} \otimes v_\gamma)$ is an eigenvector of $\boldsymbol{A}$ associated with $\lambda_\gamma \in \mathrm{spec}(A + \gamma BC)$. Thus this proves the claim. $\blacksquare$

Theorem 2 shows that the eigenvectors of $\boldsymbol{A}$ in (2) with a strictly symmetrical interconnection matrix $\varGamma$ can be classified into two types as in (17), which stem from the strict symmetry. Note that the eigenmodes of $\boldsymbol{\Sigma}$ in (1) classified into the latter of (17) are necessarily unobservable because the corresponding eigenvectors lie in $\ker \boldsymbol{C}$. These unobservable modes originate from the existence of symmetrical graph motives; Thus they appear regardless of the specific choices of system matrices. By the arguments of the dual space, we can say that uncontrollable modes appear also from the symmetry.

The eigenvectors of $\varGamma$ lying in $\mathrm{span}\{\boldsymbol{1}\}^{\perp}$ can also be deduced by analyzing the eigenspaces of $\varPi$ associated with $\pi \in \mathrm{spec}(\varPi) \setminus \{1\}$. This can be seen though the following example.

Example: Let $\varGamma$ be a symmetrical interconnection matrix. Because $\varPi \in \mathbb{P}[\varGamma]$ is simultaneously diagonalizable with $\varGamma$, the number of linearly independent eigenvectors of $\varGamma$ lying in an eigenspace of $\varPi$ coincides with the dimension of the eigenspace of $\varPi$. Therefore, if

$$\dim \ker \pi I - \varPi = 1, \quad \pi \in \mathrm{spec}(\varPi) \setminus \{1\}$$

for some $\varPi \in \mathbb{P}[\varGamma]$, then $w \in \ker \pi I - \varPi$ is an eigenvector of $\varGamma$ lying in $\mathrm{span}\{\boldsymbol{1}\}^{\perp}$. For example, the discrete Fourier transform vectors spanning $\mathrm{span}\{\boldsymbol{1}\}^{\perp}$ are the eigenvectors of both interconnection matrices $\varGamma$ in (3), because they are symmetrical with respect to the circulant permutation matrix $\varPi$ in (11), whose eigenvalues are distinct. The same argument is valid for all circulant interconnection matrices.

Next let us consider $\varGamma$ in (12), which is symmetrical with respect to $\varPi$ in (13). In this case, we have

$$\ker \pi I - \varPi = \mathrm{span}\{\mathrm{col}(0, -1, 1)\}$$

for $\pi = -1$. Thus $\mathrm{col}(0, -1, 1)$ is an eigenvector of $\varGamma$ lying in $\mathrm{span}\{\boldsymbol{1}\}^{\perp}$, which is not dependent on the parameter choice of $\mathit{\Gamma}$. From (14), we see that other two eigenvectors are given as

$$\mathrm{col}(\alpha_i, 1, 1) \in \mathrm{span}\{\mathrm{col}(1,0,0),\ \mathrm{col}(0,1,1)\}$$

where α_1 and α_2 are the solutions of

$$\alpha_i^2 + \beta^{-1}(\gamma_2 - \gamma_1)\alpha_i - 2 = 0.$$

These eigenvectors are dependent on the parameter choice of γ_i and β.

Finally, let us consider $\mathit{\Gamma}$ in (15) with $\gamma_1 = \gamma_2$, $\beta_1 = \beta_1'$, and $\beta_2 = \beta_2'$, which satisfies (9). For each permutation matrix in (16), the eigenspace $\ker \pi I - \mathit{\Pi}$ for $\pi = -1$ is obtained as

$$\begin{aligned}\mathcal{V}_1^{\perp} &:= \mathrm{span}\{\mathrm{col}(1,0,-1,0),\ \mathrm{col}(0,1,0,-1)\},\\ \mathcal{V}_2^{\perp} &:= \mathrm{span}\{\mathrm{col}(1,-1,0,0),\ \mathrm{col}(0,0,1,-1)\},\\ \mathcal{V}_3^{\perp} &:= \mathrm{span}\{\mathrm{col}(1,0,0,-1),\ \mathrm{col}(0,1,-1,0)\},\end{aligned}$$

respectively. Let us find three eigenvectors of $\mathit{\Gamma}$ such that any two of them are the elements of $\mathcal{V}_1^{\perp}$, $\mathcal{V}_2^{\perp}$, or $\mathcal{V}_3^{\perp}$. To this end, we calculate the intersections of two of them, leading to

$$\begin{aligned}&\mathrm{span}\{\mathrm{col}(1,-1,-1,1)\}, \quad \mathrm{span}\{\mathrm{col}(1,1,-1,-1)\},\\ &\mathrm{span}\{\mathrm{col}(1,-1,1,-1)\}.\end{aligned}$$

It turns out that these one-dimensional subspaces correspond to the eigenvectors of $\mathit{\Gamma}$ lying in $\mathrm{span}\{\boldsymbol{1}\}^{\perp}$. They are not dependent on the specific choice of γ_i and β_i. □

B. Aggregation of Symmetrical Graph Motives

Let ν denote the number of symmetrical graph motives, which corresponds to the size of $\mathit{\Gamma}$. As shown in Theorem 2, a set of eigenvectors of $\boldsymbol{A}$ with a strictly symmetrical interconnection matrix $\mathit{\Gamma}$ can be classified into the two types. According to this classification of eigenvectors, the eigenvalues of $\boldsymbol{A}$ can also be classified as follows.

Lemma 3: For $\boldsymbol{A}$ in (2) with $\mathit{\Gamma}$ being strictly symmetrical, it follows that

$$\mathrm{spec}(\boldsymbol{A}) = \mathrm{spec}(\hat{\boldsymbol{A}}) \cup \bigcup_{\gamma \in \mathrm{spec}(\mathit{\Gamma}) \setminus \{\gamma_0\}} \mathrm{spec}(A + \gamma BC) \quad (18)$$

where the eigenspace $\mathrm{span}\{\boldsymbol{1}\}$ of $\mathit{\Gamma}$ is associated with $\gamma_0 \in \mathrm{spec}(\mathit{\Gamma})$ and

$$\hat{\boldsymbol{A}} := \begin{bmatrix} A_0 & \sqrt{\nu} H_0 F \\ \sqrt{\nu} H F_0 & A + \gamma_0 BC \end{bmatrix}. \quad (19)$$

Furthermore, $\mathrm{col}(u, v)$ is an eigenvector of $\hat{\boldsymbol{A}}$ associated with $\lambda \in \mathrm{spec}(\hat{\boldsymbol{A}})$ if and only if $\mathrm{col}(u, \frac{1}{\sqrt{\nu}}\boldsymbol{1} \otimes v)$ is an eigenvector of $\boldsymbol{A}$ associated with λ.

Proof: From the proof of Theorem 2, we can see that

$$\lambda_\gamma \in \mathrm{spec}(A + \gamma BC)$$

is an eigenvalue of $\boldsymbol{A}$ for the eigenvalue $\gamma \in \mathrm{spec}(\mathit{\Gamma}) \setminus \{\gamma_0\}$. Furthermore, we can verify that the equality of

$$\boldsymbol{A}\,\mathrm{col}(u, \tfrac{1}{\sqrt{\nu}}\boldsymbol{1} \otimes v) = \lambda\,\mathrm{col}(u, \tfrac{1}{\sqrt{\nu}}\boldsymbol{1} \otimes v)$$

is equivalently rewritten as

$$\hat{\boldsymbol{A}}\,\mathrm{col}(u, v) = \lambda\,\mathrm{col}(u, v).$$

This proves the claim. ■

The classification of the eigenvalues of $\boldsymbol{A}$ in (18) corresponds to that of its eigenvectors in (17). From Lemma 3, we see that the multiplicity of

$$\lambda \in \textstyle\bigcup_{\gamma \in \mathrm{spec}(\mathit{\Gamma}) \setminus \{\gamma_0\}} \mathrm{spec}(A + \gamma BC) \quad (20)$$

coincides with that of $\gamma \in \mathrm{spec}(\mathit{\Gamma}) \setminus \{\gamma_0\}$. For example, the multiplicity of λ in (20) is found as $\nu - 1$ for both interconnection matrices $\mathit{\Gamma}$ in (3). As seen here, the existence of symmetrical graph motives is also relevant to the multiplicity of eigenvalues of $\boldsymbol{A}$.

Note that $\hat{\boldsymbol{A}}$ in (19) satisfies

$$\boldsymbol{A}\boldsymbol{P} = \boldsymbol{P}\hat{\boldsymbol{A}}, \quad \boldsymbol{P}^{\mathsf{T}}\boldsymbol{A} = \hat{\boldsymbol{A}}\boldsymbol{P}^{\mathsf{T}} \quad (21)$$

where the projector $\boldsymbol{P}$ such that $\boldsymbol{P}^{\mathsf{T}}\boldsymbol{P} = I$ is given by

$$\boldsymbol{P} := \mathrm{diag}\left(I, \tfrac{1}{\sqrt{\nu}}\boldsymbol{1} \otimes I\right). \quad (22)$$

Furthermore, we see that

$$\boldsymbol{B} = \boldsymbol{P}\hat{\boldsymbol{B}}, \quad \boldsymbol{C} = \hat{\boldsymbol{C}}\boldsymbol{P}^{\mathsf{T}}, \quad (23)$$

where $\hat{\boldsymbol{B}} := \boldsymbol{P}^{\mathsf{T}}\boldsymbol{B}$ and $\hat{\boldsymbol{C}} := \boldsymbol{C}\boldsymbol{P}$. On the basis of this orthogonal projection, let us consider an aggregated model of $\boldsymbol{\Sigma}$ in (1) given as

$$\hat{\boldsymbol{\Sigma}} : \begin{cases} \dot{\hat{\boldsymbol{x}}} = \hat{\boldsymbol{A}}\hat{\boldsymbol{x}} + \hat{\boldsymbol{B}}\boldsymbol{u}, & \hat{\boldsymbol{x}}(0) = \boldsymbol{P}^{\mathsf{T}}\boldsymbol{x}_0 \\ \hat{\boldsymbol{y}} = \hat{\boldsymbol{C}}\hat{\boldsymbol{x}}. \end{cases} \quad (24)$$

This aggregated model is *almost equivalent* to the original system in the following sense.

Theorem 4: For $\boldsymbol{\Sigma}$ in (1) with $\mathit{\Gamma}$ being strictly symmetrical, let $\hat{\boldsymbol{\Sigma}}$ be defined as in (24). Then

$$\boldsymbol{y}(t) \equiv \hat{\boldsymbol{y}}(t), \quad t \geq 0 \quad (25)$$

for any $\boldsymbol{x}_0$ and $\boldsymbol{u}$. In particular, if $\boldsymbol{x}_0 \in \mathrm{im}\,\boldsymbol{P}$, then

$$\boldsymbol{x}(t) \equiv \boldsymbol{P}\hat{\boldsymbol{x}}(t), \quad t \geq 0. \quad (26)$$

Furthermore, $\boldsymbol{\Sigma}$ is detectable (stabilizable) if and only if $\hat{\boldsymbol{\Sigma}}$ is detectable (stabilizable) and $A + \gamma BC$ is stable for all $\gamma \in \mathrm{spec}(\mathit{\Gamma}) \setminus \{\gamma_0\}$.

Proof: For any $\boldsymbol{x}_0$ and $\boldsymbol{u}$, we have

$$\boldsymbol{x}(t) = \exp(\boldsymbol{A}t)\boldsymbol{x}_0 + \int_0^t \exp(\boldsymbol{A}(t-\tau))\boldsymbol{B}\boldsymbol{u}(\tau)d\tau.$$

From the second relations in (21) and (23), we see that

$$\boldsymbol{C}\boldsymbol{A}^k = \hat{\boldsymbol{C}}\hat{\boldsymbol{A}}^k\boldsymbol{P}^{\mathsf{T}}$$

for any natural number k. Thus (25) is proven by

$$\boldsymbol{C}\exp(\boldsymbol{A}t) = \hat{\boldsymbol{C}}\exp(\hat{\boldsymbol{A}}t)\boldsymbol{P}^{\mathsf{T}}.$$

Furthermore, from the first relations in (21) and (23), it follows that

$$\boldsymbol{A}^k\boldsymbol{B} = \boldsymbol{P}\hat{\boldsymbol{A}}^k\hat{\boldsymbol{B}},$$

which leads to

$$\exp(\boldsymbol{A}t)\boldsymbol{B} = \boldsymbol{P}\exp(\hat{\boldsymbol{A}}t)\hat{\boldsymbol{B}}.$$

From $\boldsymbol{x}_0 = \boldsymbol{P}\boldsymbol{P}^{\mathsf{T}}\boldsymbol{x}_0$ for $\boldsymbol{x}_0 \in \operatorname{im}\boldsymbol{P}$, we have (26).

Next we show the relation of detectability. From Theorem 2 and Lemma 3, we see that the unobservable modes of $\boldsymbol{\Sigma}$ eliminated by the aggregation of $\boldsymbol{P}$ are associated with the eigenvalues of λ in (20). Thus the unobservable modes are stable by the assumption that $A + \gamma BC$ is stable for all $\gamma \in \operatorname{spec}(\mathit{\Gamma}) \setminus \{\gamma_0\}$. The claim of stabilizability can be shown by the same arguments of the dual space. ■

As shown in (25), the aggregated model $\hat{\boldsymbol{\Sigma}}$ has the same initial value response as well as input-to-output characteristics as those of the original system $\boldsymbol{\Sigma}$. This stems from the *unobservability* of symmetrical graph motives. On the other hand, the property of state trajectories in (26) stems from their *uncontrollability*. Both properties of (25) and (26) are, in principle, essential for designing an observer-based state feedback controller when utilizing the aggregated model. This is because, unless (25) holds, there can be discrepancy in the measurement output that is injected to an observer; on the other hand, unless (26) holds, there can be discrepancy in an observed state that is fedback to the plant as a control input signal. As a relaxation of this, some small approximation errors can be taken into account in a robust control framework.

IV. Numerical Demonstration

A. Second-Order Oscillator Network

Let us consider a network system depicted as the upper graph in Fig. 3, which is composed of three large nodes forming a chain and 30 small nodes forming a circle. In this section, regarding each node as a second-order oscillator, i.e., a mass-spring-damper system, we consider an output regulation problem of the oscillator network. This kind of second-order networks is called a (linearized) swing equation in power systems control [11]. A similar loop-topology model can be found in [19], [20], for which a stability analysis is performed from a viewpoint of node coherence.

The system dynamics is given as follows. Let $\mathcal{L}$ denote the unweighted symmetric graph Laplacian matrix compatible with the upper graph in Fig. 3. In particular, the $(1,1)$-block of $\mathcal{L}$ is given as

$$\mathcal{L}_{11} = \begin{bmatrix} 1 & -1 & 0 \\ -1 & 2 & -1 \\ 0 & -1 & 31 \end{bmatrix},$$

which corresponds to the chain of large nodes. Using this matrix, we obtain the $(1,1)$-block of $\boldsymbol{A}$ in (2) as

$$A_0 = I \otimes \begin{bmatrix} 0 & 1 \\ 0 & -\frac{d}{M} \end{bmatrix} - \mathcal{L}_{11} \otimes \begin{bmatrix} 0 \\ \frac{1}{M} \end{bmatrix} \begin{bmatrix} k & 0 \end{bmatrix}$$

where $M > 0$ denotes a mass constant, $d > 0$ denotes a damper constant, and $k > 0$ denotes a spring constant. In a similar way, the $(1,2)$-block of $\boldsymbol{A}$ is given as

$$H_0(\boldsymbol{1}^{\mathsf{T}} \otimes F) = \mathcal{L}_{12} \otimes \begin{bmatrix} 0 \\ \frac{1}{M} \end{bmatrix} \begin{bmatrix} k & 0 \end{bmatrix},$$

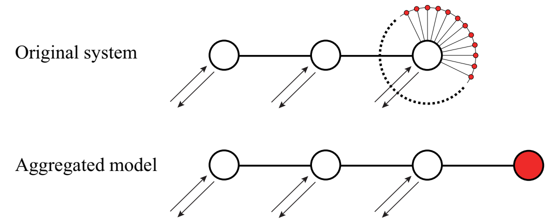

Fig. 3. Network structures of original system and aggregated model.

where $\mathcal{L}_{12} = \operatorname{col}(0,0,1)\boldsymbol{1}^{\mathsf{T}}$. This leads to

$$H_0 = \operatorname{col}(0,0,1) \otimes \begin{bmatrix} 0 \\ \frac{1}{M} \end{bmatrix}, \quad F = \begin{bmatrix} k & 0 \end{bmatrix}.$$

The $(2,2)$-block of $\mathcal{L}$ is given as the symmetric circulant matrix

$$\mathcal{L}_{22} = C_{30} + C_{30}^{\mathsf{T}}, \quad C_{30} := I - (e_1 e_2^{\mathsf{T}} + \cdots + e_{30} e_1^{\mathsf{T}}),$$

which corresponds to the circle of small nodes. In this notation, the $(2,2)$-block of $\boldsymbol{A}$ corresponding to the network of symmetrical graph motives can be represented as

$$\begin{aligned} A &= \begin{bmatrix} 0 & 1 \\ 0 & -\frac{d}{m} \end{bmatrix}, & B &= \begin{bmatrix} 0 \\ \frac{1}{m} \end{bmatrix} \\ C &= \begin{bmatrix} \delta & k \end{bmatrix}, & \mathit{\Gamma} &= -\mathcal{L}_{22}, \end{aligned} \tag{27}$$

where $m > 0$ denotes a mass constant for small nodes and $\delta \geq 0$ denotes a coefficient of coupling among small nodes. Then, in a way similar to the $(1,2)$-block of $\boldsymbol{A}$, the $(2,1)$-block can be represented by

$$F_0 = \operatorname{col}^{\mathsf{T}}(0,0,1) \otimes \begin{bmatrix} k & 0 \end{bmatrix}, \quad H = \begin{bmatrix} 0 \\ \frac{1}{m} \end{bmatrix}.$$

Finally, $\boldsymbol{B}$ and $\boldsymbol{C}$ in (2) are given with

$$B_0 = I \otimes \begin{bmatrix} 0 \\ 1 \end{bmatrix}, \quad C_0 = I \otimes \begin{bmatrix} 1 & 0 \end{bmatrix},$$

which imply that the input signals are injected to all large nodes and the output signals are measured as their positions. These system matrices lead to a 66-dimensional network system $\boldsymbol{\Sigma}$ in (1). This system is semistable and has one zero eigenvalue for any choice of constants. Furthermore, for any constant input signal, it follows that

$$\boldsymbol{x}_3^* = \boldsymbol{x}_4^* = \cdots = \boldsymbol{x}_{33}^*,$$

where $\boldsymbol{x}_i^*$ denotes the steady state of the ith node. This implies that all states of small nodes are to be synchronized with that of the third large node. The values of $\boldsymbol{x}_1^*$, $\boldsymbol{x}_2^*$, and $\boldsymbol{x}_3^*$ can vary with the value of input signals.

B. Output Regulator Design Based on Aggregated Model

To design an output regulator for the network system $\boldsymbol{\Sigma}$, let us utilize the aggregated model $\hat{\boldsymbol{\Sigma}}$ in (24), whose network structure is depicted as the lower graph in Fig. 3. In particular, regarding $\hat{\boldsymbol{\Sigma}}$ as a plant to be controlled, we consider designing an observer-based integrator in the form of

$$\boldsymbol{\Xi} : \begin{cases} \dot{\hat{\boldsymbol{\xi}}} = \hat{\boldsymbol{A}}\hat{\boldsymbol{\xi}} + \hat{\boldsymbol{B}}\boldsymbol{u} + \hat{\boldsymbol{H}}(\hat{\boldsymbol{y}} - \hat{\boldsymbol{C}}\hat{\boldsymbol{\xi}}) \\ \dot{\lambda} = \boldsymbol{y}^* - \hat{\boldsymbol{C}}\hat{\boldsymbol{\xi}}, \end{cases} \tag{28}$$

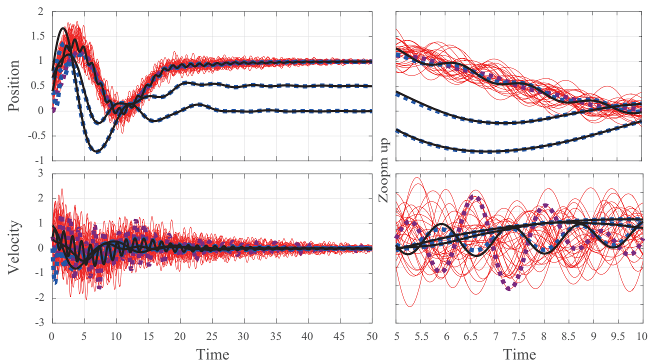

Fig. 4. Output regulation of network system with $\delta = 0$.

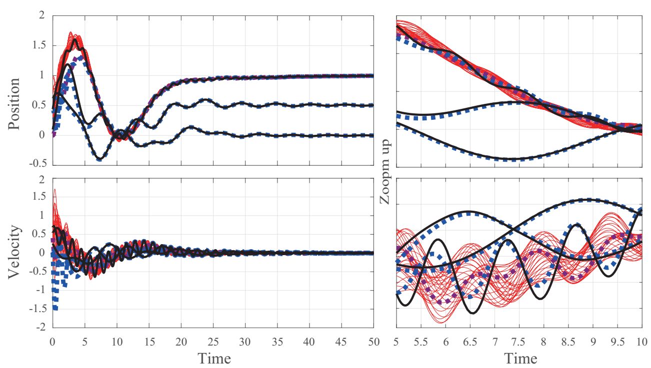

Fig. 5. Output regulation of network system with $\delta = 1$.

where the first dynamics corresponds to the observer of $\hat{\boldsymbol{\Sigma}}$, which is eight-dimensional, and the second is the three-dimensional integrator for output regulation, steering the system output to a reference signal denoted by $\boldsymbol{y}^*$. Note that the measurement signal $\hat{\boldsymbol{y}}$ in the observer can be equivalently replaced with the system output $\boldsymbol{y}$ owing to the property of (25). On the premise of the feedback control of

$$\boldsymbol{u} = \hat{\boldsymbol{K}}\hat{\boldsymbol{\xi}} + K\lambda,$$

the output regulation

$$\lim_{t\to\infty} \boldsymbol{y} = \boldsymbol{y}^*$$

is achieved if the feedback gains are designed such that

$$\begin{bmatrix} \hat{\boldsymbol{A}} & 0 \\ -\hat{\boldsymbol{C}} & 0 \end{bmatrix} + \begin{bmatrix} \hat{\boldsymbol{B}} \\ 0 \end{bmatrix} \begin{bmatrix} \hat{\boldsymbol{K}} & K \end{bmatrix}, \quad \hat{\boldsymbol{A}} - \hat{\boldsymbol{H}}\hat{\boldsymbol{C}} \tag{29}$$

are stable. Note that the four-dimensional observer works as an average state observer of $\boldsymbol{\Sigma}$, which attains

$$\lim_{t\to\infty} \begin{bmatrix} \hat{\boldsymbol{\xi}}_1 - \boldsymbol{x}_1 \\ \hat{\boldsymbol{\xi}}_2 - \boldsymbol{x}_2 \\ \hat{\boldsymbol{\xi}}_3 - \boldsymbol{x}_3 \\ \hat{\boldsymbol{\xi}}_4 - \frac{1}{\sqrt{30}}(\boldsymbol{x}_4 + \cdots + \boldsymbol{x}_{33}) \end{bmatrix} = 0. \tag{30}$$

This is owing to the property of (26).

C. Numerical Experiments

In the following, we set the system parameters as

$$M = 10, \quad m = 1, \quad k = 5, \quad d = 0.1.$$

In this setting, we investigate two cases of $\delta = 0$ and $\delta = 1$ in (27). A set of stabilizing gains in (29) is found by the standard LQR design technique. Furthermore, the output reference signal is given as

$$\boldsymbol{y}^* = \mathrm{col}(0, 0.5, 1),$$

which implies that the positions of three large nodes are to be steered to 0, 0.5, and 1, respectively. The initial value of $\boldsymbol{\Sigma}$ is given randomly.

For $\delta = 0$, the trajectories of the network system $\boldsymbol{\Sigma}$ and its average state observer in $\boldsymbol{\Xi}$ in (28) are shown in Fig. 4, where the black thick lines correspond to the states of large nodes, the red thin lines correspond to those of small nodes, and the dotted lines correspond to those of the observer. The observer state variable $\hat{\boldsymbol{\xi}}_4$ is scaled by $\frac{1}{\sqrt{30}}$ as being compatible with (30). From this figure, we can see that the states of three large nodes are steered to the target positions while the states of the average state observer track the centroids of the system states in the sense of (30).

For $\delta = 1$, the resultant trajectories are shown in Fig. 5, where the same notation as Fig. 4 is used. In this case, the synchronization of small nodes becomes stronger than the previous case because the value of δ works as a damper coefficient for the reduction of discrepancy among small nodes. These results demonstrate that the observer-based state feedback controller design based on aggregated models works well and it is reasonable for network systems having a number of symmetrical graph motives, whose states are to be synchronized with each other.

V. Concluding Remarks

In this paper, from a viewpoint of the symmetry of graph motives, we have analyzed a sparse structure appearing in eigenvectors, i.e., eigenmodes of network systems. Furthermore, this eigenstructure analysis has been applied to reduced order controller design based on aggregated models, derived by aggregating symmetrical graph motives. It has been found that the existence of symmetry, formulated as the graph automorphism, makes a local state space associated with the motives both uncontrollable and unobservable. An aggregated model given by removing the redundant modes is useful in designing a state feedback controller composed of an average state observer, which tracks a kind of centroids of the system states.

As a numerical demonstration of the aggregated controller design, we have performed output regulation of a second-order oscillator network. Our aggregated controller design is based on the premise that the aggregated model is both controllable and observable, whereas the original oscillator network is supposed to be only stabilizable and detectable. In particular, the original is supposed to involve a number of particular uncontrollable and unobservable modes that correspond to the disagreement with the average of the state space associated with symmetrical graph motives. The degree of stability of disagreement modes is relevant to the *coherence* of symmetrical graph motives. From this viewpoint, we see that making explicit use of the redundancy from graph symmetry, e.g., sensor and actuator allocation with explicit consideration of coherent states (cluster states), can be a key insight into reasonably controlling large-scale network systems. Introducing a notion of approximation in the construction of aggregated models, in a way of [16], [17], would be worth pursuing to make the aggregated controller design method more practical.

ACKNOWLEDGMENTS

This research was supported in part by CREST, JST, and by JSPS Grant-in-Aid for Young Scientists (B) Grant Number 26820165.

REFERENCES

[1] M. Newman, *Networks: an introduction*. Oxford University Press, 2009.

[2] S. H. Strogatz, "Exploring complex networks," *Nature*, vol. 410, no. 6825, pp. 268–276, 2001.

[3] U. Alon, "Network motifs: theory and experimental approaches," *Nature Reviews Genetics*, vol. 8, no. 6, pp. 450–461, 2007.

[4] R. Milo, S. Shen-Orr, S. Itzkovitz, N. Kashtan, D. Chklovskii, and U. Alon, "Network motifs: simple building blocks of complex networks," *Science*, vol. 298, no. 5594, pp. 824–827, 2002.

[5] F. Chung, L. Lu, T. G. Dewey, and D. J. Galas, "Duplication models for biological networks," *Journal of computational biology*, vol. 10, no. 5, pp. 677–687, 2003.

[6] B. D. MacArthur, R. J. Sánchez-García, and J. W. Anderson, "Symmetry in complex networks," *Discrete Applied Mathematics*, vol. 156, no. 18, pp. 3525–3531, 2008.

[7] B. Noble and J. W. Daniel, *Applied linear algebra*. Prentice-Hall New Jersey, 1988, vol. 3.

[8] M. Mesbahi and M. Egerstedt, *Graph theoretic methods in multiagent networks*. Princeton University Press, 2010.

[9] B. D. MacArthur and R. J. Sánchez-García, "Spectral characteristics of network redundancy," *Physical Review E*, vol. 80, no. 2, p. 026117, 2009.

[10] A. Pogromsky, G. Santoboni, and H. Nijmeijer, "Partial synchronization: from symmetry towards stability," *Physica D: Nonlinear Phenomena*, vol. 172, no. 1, pp. 65–87, 2002.

[11] J. Zhou and Y. Ohsawa, "Improved swing equation and its properties in synchronous generators," *Circuits and Systems, IEEE Transactions on*, vol. 56, no. 1, pp. 200–209, 2009.

[12] A. Rahmani, M. Ji, M. Mesbahi, and M. Egerstedt, "Controllability of multi-agent systems from a graph-theoretic perspective," *SIAM Journal on Control and Optimization*, vol. 48, no. 1, pp. 162–186, 2009.

[13] M. Egerstedt, "Controllability of networked systems," in *Mathematical Theory of Networks and Systems*, 2010.

[14] Y.-Y. Liu, J.-J. Slotine, and A.-L. Barabási, "Controllability of complex networks," *Nature*, vol. 473, no. 7346, pp. 167–173, 2011.

[15] M. Bürger, D. Zelazo, and F. Allgöwer, "Hierarchical clustering of dynamical networks using a saddle-point analysis," *Automatic Control, IEEE Transactions on*, vol. 58, no. 1, pp. 113–124, 2013.

[16] T. Ishizaki, K. Kashima, J.-i. Imura, and K. Aihara, "Model reduction and clusterization of large-scale bidirectional networks," *Automatic Control, IEEE Transactions on*, vol. 59, no. 1, pp. 48–63, 2014.

[17] T. Ishizaki, K. Kashima, A. Girard, J.-i. Imura, L. Chen, and K. Aihara, "Clustered model reduction of positive directed networks," *Automatica*, vol. 59, pp. 238–247, 2015.

[18] D. S. Bernstein, *Matrix mathematics: theory, facts, and formulas*. Princeton University Press, 2009.

[19] Y. Susuki, I. Mezić, and T. Hikihara, "Coherent swing instability of power grids," *Journal of nonlinear science*, vol. 21, no. 3, pp. 403–439, 2011.

[20] ——, "Coherent swing instability of power systems and cascading failures," in *Power and Energy Society General Meeting, 2010 IEEE*. IEEE, 2010, pp. 1–8.